Theoretical Physics

A Study of Josephson Junction Characteristics

Björn Ahlgren (900627-1275)
bjornah@kth.se Tel. 070-3862765
Studentbacken 25 lgh1410, 115 57 Stockholm

David Byström (890307-7496)
dby@kth.se Tel. 073-0227932
Gryningsvägen 27, 142 42 Skogås

SA104X Degree Project in Engineering Physics, First Level
Department of Theoretical Physics
Royal Institute of Technology (KTH)
Supervisor: Patrik Henelius

May 13, 2011

Abstract

This Bachelor thesis has as its aim to investigate Josephson junctions by examining their I-V characteristics and to visualize various phenomena associated with Josephson junctions. Primarily, everything considered in this thesis uses a semi-classical model where quantum effects have been excluded. The thesis focuses on 1D arrays of Josephson junctions fed with direct current with the goal to study what occurs when many junctions are placed in a row. First a single Josephson junction is simulated and we observe a hysteresis in the I-V characteristics that is examined. Secondly a 1-D array is considered and the coupled system of differential equations that follows is solved numerically, and from this data the properties of Josephson junctions are deduced. We discovered that this array generally has similar properties to a single Josephson junction. We also sought to replicate results obtained experimentally in the lab by David Haviland and his co-workers at KTH, but by simulations, to see how good our models are. We have produced data agreeing partly with the experimental results and we have had no directly contradicting outcomes from our simulations. An explicit relation between the number of Josephson junctions and the feature of the I-V characteristics was derived and the validity of our model was strengthened by the consistency of our results.

Sammanfattning

Målet med denna avhandling är att undersöka så kallade Josephson junctions genom att studera deras I-V-karaktäristiker, samt att visualisera diverse fenomen associerade med dessa. Primärt i denna avhandling används en semiklassisk model där kvanteffekter i hög grad bortses ifrån. Avhandlingen fokuserar på kedjor av seriekopplade Josephson junctions vilka matas med likström, med syftet att utforska vad som sker då ett stort antal kretsar kopplas samman. Först simuleras en ensam Josephson junction varpå vi observerar hysteres i I-V-karaktäristiken. En kedja med Josephson junctions betraktas sedan och det system med kopplade, ickelinjära differentialekvationer som beskriver matrisen, löses numeriskt och ur dessa data finner man egenskaperna hos kretsen. Vi fann att denna kedja generellt sett har samma egenskaper som en ensam Josephson junction. Även att återskapa resultat från experiment genomförda i ett laboratorium på KTH har varit ett mål, vilket till viss del har lyckats. Våra modeller återspeglar verkligheten under de förutsättningar vi testat dem. Vi har med hjälp av dessa modeller härlett ett explicit samband mellan antalet Josephson junctions och utseendet på I-V karaktäristiken.

Contents

Chapter 1

Introduction

The aim of this thesis is to examine Josephson junctions and their I-V characteristics. Especially 1-D arrays of Josephson junctions will be examined. Also, we will try to replicate results obtained in the lab by David Haviland and his co-workers at KTH, specifically a certain I-V characteristic found when having a large number of Josephson junctions in a 1-D array.

A Josephson junction is a small, very sensitive circuit that combines supercurrents with the quantum phenomena of tunneling of coupled electrons which lead to a current flowing in the circuit. The symbol of the circuit, when drawn in a circuit diagram, is an X, see Fig. 1.1. The circuit works by the Josephson effect which has found its way into several applications in modern technology. Since frequency is defined in a precise manner, it is convenient to use the Josephson effect to define the voltage due to its highly sensitive voltage-frequency dependence. There are several variants to superconducting tunnel junctions but for simplicity we will confine ourselves to Josephson junctions in this text and we will also refer to all superconducting tunnel junctions as Josephson junctions if there are no special conditions requiring anything else. The background theory as well as the terminology will be presented to the reader in Chapter 2; Background.

Figure 1.1: Schematic picture of a Josephson junction.

1.1 History

The Josephson effect is named after Brian D. Josephson due to his prediction of the phenomena in 1962, which earned him the Nobel Prize 1973. The paper predicted that a current can flow through a circuit consisting of two superconducting metals, separated by a thin insulating film Ref. [4]. This effect has since been verified by numerous experiments and is today a well established phenomenon. The first Josephson junction, essentially a simple tunnel junction named after the origin of its function, was constructed as soon as the following year, 1963, by John Rowell and Philip Anderson at Bell Labs Ref. [1].

1.2 Applications

As with most scientific discoveries, applications eventually turn up and Josephson junctions are no exception. One of the first applications was the definition of the volt, since this could be measured very precisely with Josephson junctions. It was discovered in 1964 that the I-V characteristics of a Josephson junction, irradiated by electro-magnetic waves of frequency f, exhibits so called "Shapiro steps" at voltages an integer times the quantum flux constant Φ_0 divided by the frequency Ref. [6](pg 202-204). Since the frequency is the most precisely measured quantity as of today, it allows volt measurements with excellent accuracy. This was the reason for the definition of the volt using Josephson junctions. However, this is no longer the definition of a volt, but it is still a good way to calibrate voltmeters.

1.2.1 SQUIDs

A superconducting quantum interference device, or a SQUID, is a device that has found its way into many applications as it is highly sensitive to magnetic fields and can measure fields as weak as $5 \cdot 10^{-11}$ G/Hz$^{-1/2}$ Ref. [6](pg 232). The SQUID is basically two parallel Josephson junctions that forms a superconducting loop which magnetic fields can pass through. This in turn affects, in a very delicate way, how the current through the DC SQUID flows; a feature that makes it ideal to measure magnetic fields. A SQUID is depicted in Fig. 1.2. SQUIDs are used in a variety of fields such as the field of biology, where they are used in Magnetoencephalography to give information about the neural activity inside brains. They are also used in different apparatus to measure the magnetic properties of material samples.

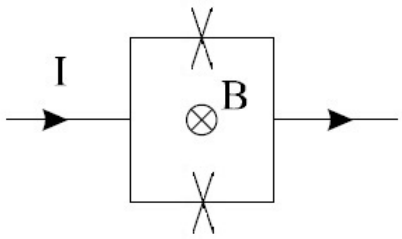

Figure 1.2: A simple model of a SQUID; two parallel connected Josephson junctions encloses a magnetic flux.

1.2.2 In the future

A possible future application of Josephson junctions is in quantum computing. A certain type of quantum bit, the flux qubit, consists of small loops of superconducting metal separated by a number of Josephson junctions. SQUIDs may also be used in the manufacturing of quantum bits. Since the scope of this text is the Josephson junctions themselves, we leave this exciting research field here and focus instead on the work of this thesis.

Chapter 2

Background

Here we expound the material we have used in this thesis and present the reader with many of our references and the basic concepts of Josephson junctions as well as the Josephson effect.

2.1 Superconductivity

1911 Kamerlingh Onnes observed how the electrical resistance for some metals went to zero as it was cooled down below some material specific critical temperature T_c. That was the discovery of superconductivity. Superconductivity is not the scope of this thesis, but it is nevertheless good if the reader has at least a basic understanding of its principles, since it plays a vital role in the underlying physics in this thesis.

There are several ways to characterize superconductivity; its first observed property is that a superconductor is a perfect conductor, we thus have no loss in current or magnetic field produced by the current in a superconductor. In fact one expects no loss in up to $10^{10^{10}}$ years, depending on the type of superconductor. The second effect of superconductivity to be discovered was perfect diamagnetism, discovered in 1933 by Meissner and Ochsenfeld. It was shown that magnetic fields are expelled from superconductors as they are cooled below T_c, which is known as the Meissner effect. This also implies that superconductivity could be destroyed by a strong magnetic field, which turns out to be the case. When a superconductor is placed in the critical field H_c the superconductivity will disappear. There are two types of superconductors, type I and type II, that differ in how they react to magnetic fields approaching H_c. A type I superconductor will not change its properties at all until it has a discontinuous breakdown at H_c, while a type II superconductor will have an increasing inner flux from a lower critical field H_{c1} to H_{c2} where it too breaks down, but continuously, see Fig. 2.1. The type II superconductor creates a vortex array giving rise to a quantity known as *quantum flux*

$$\Phi_0 = \frac{hc}{2e}, \tag{2.1}$$

where e is the elementary charge, h is Planck's constant and c is the speed of light. This quantity will be important to us later but we will not derive it here.

Another important feature is that there exists a macroscopic, many-particle wave function $\Phi(\mathbf{r})$. This wave function, with a phase and amplitude, resembles the Bose-Einstein condensate by the fact that it maintains its phase over macroscopic distances.

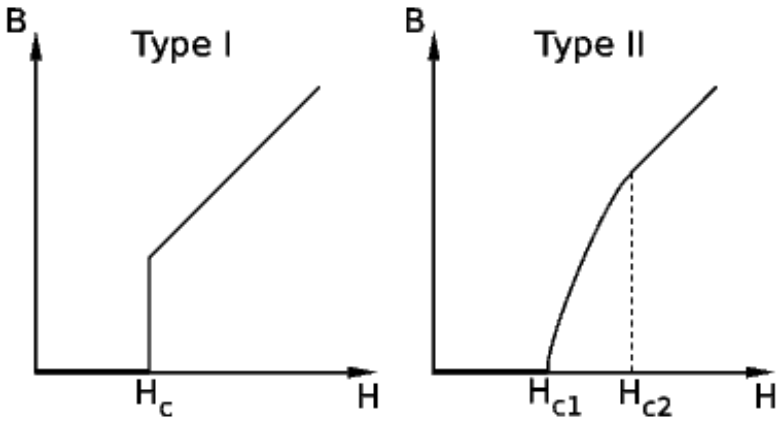

Figure 2.1: Internal magnetic field when submitted to an external magnetic field H of a type I and type II superconductor respectively.

While there are single bosons in the Bose-Einstein condensate, there are so called *Cooper pairs* of electrons in the superconductor.

Cooper pairs are quasiparticles consisting of two electrons, one in a state $-\mathbf{k}\downarrow$ and one in the state $\mathbf{k}\uparrow$, which, when treated as a quasiparticle, function as a boson, thus enabling the particles to all inhabit the lowest energy level and to share the characteristic macroscopic wave function. The square of the wave function $|\psi|^2$ is the electron density n. Therefore, the wave function can be described as $\psi = n^{1/2}e^{i\theta}$, where θ is the phase of the wave function. Ref. [6](Chapter 1)

2.2 Quantum Tunneling

Quantum tunneling is another physical phenomena that is vital to the underlying physics of this thesis. The principle is that a quantum particle can enter zones 'forbidden' by classical physics.

Quantum particles are described by wave functions. Classically described free particles are hindered by potential barriers and can only be located in areas that they have the kinetic energy to reach. This is not the case for quantum particles. The fact that they are described by wave functions, and not by a single position, allow them to enter areas of higher potential. This allows them to tunnel through areas of high potential, where classical particles would simply bounce back.

2.3 Josephson Junction

Here we give the reader all the information about Josephson junctions needed, starting with the crucial Josephson effect. We then move on to model Josephson junctions and look at their theoretical properties.

2.3.1 Josephson effect

The Josephson effect is the physical phenomena describing what occurs when we have quantum tunneling between superconductors. This effect can be derived as follows: Ref. [5]

Let ψ_1 be the probability amplitude for electron pairs to be on one side of a junction while ψ_2 is the probability amplitude for electron pairs to be on the other side of the junction. Then the time-dependent Schrödinger equation, $i\hbar\frac{\partial\Psi}{\partial t} = \hat{H}\Psi$, applied to the two amplitudes gives

$$i\hbar\frac{\partial\psi_1}{\partial t} = \hbar T\psi_2; \qquad i\hbar\frac{\partial\psi_2}{\partial t} = \hbar T\psi_2, \tag{2.2}$$

where $\hbar T$ represents the effect of the electron-pair coupling or transfer interaction across the insulator. T is a measure of the leakage of ψ_1 into region 2 and of ψ_2 into region 1. As stated in section 2.1, the wave function in each region can be described as $\psi_1 = n_1^{1/2}e^{i\theta_1}$ and $\psi_2 = n_2^{1/2}e^{i\theta_2}$. Then

$$\frac{\partial\psi_1}{\partial t} = \frac{1}{2}n_1^{-1/2}e^{i\theta_1}\frac{\partial n_1}{\partial t} + i\psi_1\frac{\partial\theta_1}{\partial t} = -iT\psi_2; \tag{2.3}$$

$$\frac{\partial\psi_2}{\partial t} = \frac{1}{2}n_2^{-1/2}e^{i\theta_2}\frac{\partial n_2}{\partial t} + i\psi_2\frac{\partial\theta_2}{\partial t} = -iT\psi_1. \tag{2.4}$$

If we multiply the first of the two equations by $n_1^{1/2}e^{-i\theta_1}$ and the second by $n_2^{1/2}e^{-i\theta_2}$, we obtain, with $\delta \equiv \theta_2 - \theta_1$

$$\frac{1}{2}\frac{\partial n_1}{\partial t} + in_1\frac{\partial\theta_1}{\partial t} = -iT(n_1n_2)^{1/2}e^{i\delta}; \tag{2.5}$$

$$\frac{1}{2}\frac{\partial n_2}{\partial t} + in_2\frac{\partial\theta_2}{\partial t} = -iT(n_1n_2)^{1/2}e^{-i\delta}. \tag{2.6}$$

We now equate the real and imaginary parts on the left and the right side of these equations and attain

$$\frac{\partial n_1}{\partial t} = 2T(n_1n_2)^{1/2}\sin\delta; \qquad \frac{\partial n_2}{\partial t} = -2T(n_1n_2)^{1/2}\sin\delta; \tag{2.7}$$

$$\frac{\partial\theta_1}{\partial t} = -T\left(\frac{n_2}{n_1}\right)^{1/2}\cos\delta; \qquad \frac{\partial\theta_2}{\partial t} = -T\left(\frac{n_1}{n_2}\right)^{1/2}\cos\delta. \tag{2.8}$$

If the superconductors in region 1 and 2 are identical, then $n_1 = n_2$ and Eq. (2.8) imply that

$$\frac{\partial\theta_1}{\partial t} = \frac{\partial\theta_2}{\partial t}; \qquad \frac{\partial}{\partial t}(\theta_2 - \theta_1) = 0, \tag{2.9}$$

while Eq. (2.7) imply that

$$\frac{\partial n_2}{\partial t} = -\frac{\partial n_1}{\partial t}. \tag{2.10}$$

The current flow is proportional to $\frac{\partial n_2}{\partial t}$ or, $-\frac{\partial n_1}{\partial t}$. From Eq. (2.7) we can conclude that the current I is dependent only on the phase difference δ, as

$$I = I_c\sin\delta \tag{2.11}$$

where I_c is proportional to the transfer interaction T.

2.3.2 The RCSJ model

In order to better describe a real tunnel junction, taking into account the fact that a real junction is not perfect, we may use the RCSJ, resistivity and capacitively shunted junction, model. Ref. [6](pg 211-212) This model models the Josephson junction as three parallel circuits; a capacitor to simulate the geometrically induced capacitance between the electrodes in the junction, a resistance to account for dissipation when we have a finite voltage and, the Josephson junction itself in its ideal version.

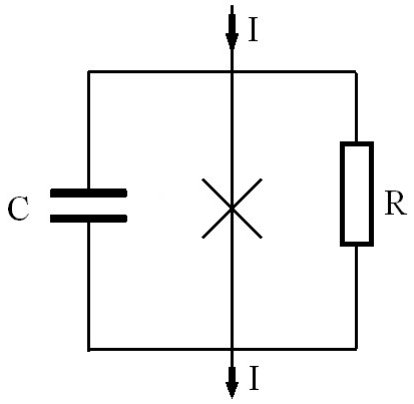

Figure 2.2: The equivalent circuit of the RCSJ model. The Josephson junction's non-ideal nature, is modeled by inserting the ideal Josephson junction into a circuit where it is parallel connected to a capacitor with capacitance C and a resistor with resistance R.

2.3.3 The tilted washboard model

A way to illustrate the phase of a Josephson junction as well as the voltage and current, is by using the tilted washboard model. In this mechanical analogue of a Josephson junction, we imagine a ball-shaped mass resting on a washboard; that is a large, periodically deformed surface, depicted in cross-section in the left top corner of Fig. 2.3. γ in the graphs are the angle in radians of the potential. In this analogue the current is the slope of the washboard and the velocity of the mass over the washboard is interpreted as the voltage over the junction. In this model we assign some friction to the movement of the mass (equivalent of the resistance in the junction). With no incline of the washboard we will of course have no movement of the mass, that is, no voltage. When the washboard is given some incline according to Fig. 2.3, the mass will still be at rest in the small valleys if the washboard is tilted slowly so that the mass can be considered almost at rest during the process of tilting the board. That we can have an inclined plane with a zero velocity for the mass is analogous to the superconductivity of the junctions when the current is below the critical current I_c. When the angle is increased to the critical angle, representing the critical current I_c, as in the bottom right corner of Fig. 2.3, there remains no valleys to keep the mass from moving. There will thus be movement of the mass (voltage), when the critical angle (current) has been reached.

The analogue has other possible uses as well, especially in simulation where the speed of the tilting can be thought of as related to over how long time we must solve the

differential equations in order to obtain stability, but that will be discussed in later chapters.

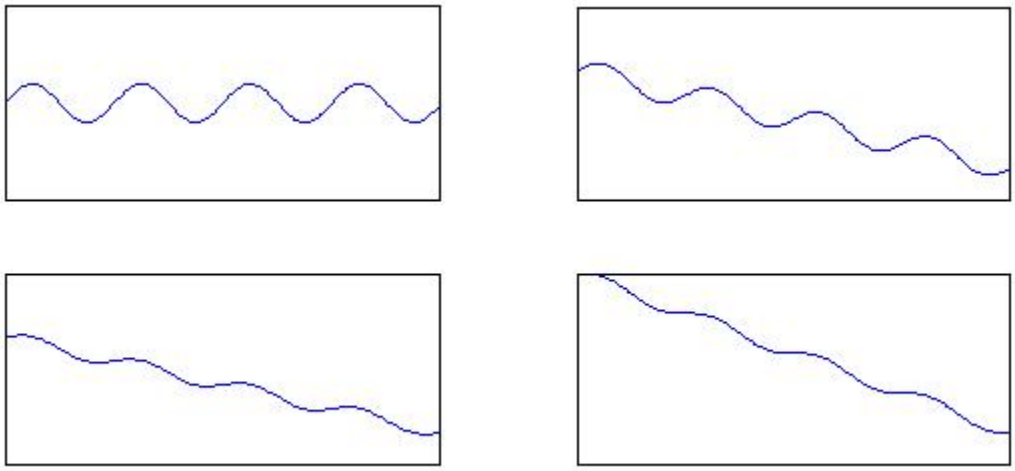

Figure 2.3: The washboard model of the Josephson effect depicts the current as the movement of a mass over the washboard. An incline of the plane but with valleys remaining for the mass to rest in represents a superconducting state of the junction. When a certain angle is reached, analogous to the critical current I_c, there remains no potentials where the mass can be at rest and it will thus have a velocity, representing the voltage appearing in the junction.

Chapter 3

Investigation

The purpose of this bachelor thesis is to model Josephson junctions coupled in series using the RCSJ model and look at the I-V characteristics that such an array displays. The results are compared to what would be expected theoretically and what is obtained experimentally. The effects on the I-V characteristics when the number of Josephson junctions change is also considered.

3.1 Experimental Background

There have been extensive experimental studies of Josephson junctions. These experimental results are what we are comparing our simulations to, specifically results by David Haviland and his reasearch group at KTH, Stockholm, Sweden. One example of a typical hysteresis curve of a 1D-array of Josephson junctions can be found in Fig. 3.1, which is a graph corresponding to 255 Josephson junctions in a series.

Apart from wanting consistency with experimental results, we will investigate more closely if there are some explicit connection between the shape and behavior of the I-V characteristics, and the number of Josephson junctions and the parameters β_c and the critical current I_c.

3.2 Model

The Josephson junction is modeled as three parallel devices, one resistor, one capacitance and one tunneling device. Kirchoff's law states that the total current out is the same as the total current in at a junction, hence, a total current in I will split between the three parallel components dependent on their type; $I = I_{res} + I_{cap} + I_{tun}$.

I_{res} is the current through the resistor, I_{cap} is the current through the capacitor while I_{tun} is the current through the tunneling device. We know that $I_{res} = \frac{V}{R}$. The current through the capacitor can be derived from the definition of capacitance,

$$Q = CV \rightarrow \frac{dQ}{dt} = C\frac{dV}{dt} \rightarrow I_{cap} = C\frac{dV}{dt}. \tag{3.1}$$

The tunneling current was derived in section 2.3.1 and was found to be $I_{tun} = I_c \sin(\varphi)$. This gives an equation that relates current to the voltage and phase shift,

$$I = \frac{V}{R} + C\frac{dV}{dt} + I_c \sin(\varphi). \tag{3.2}$$

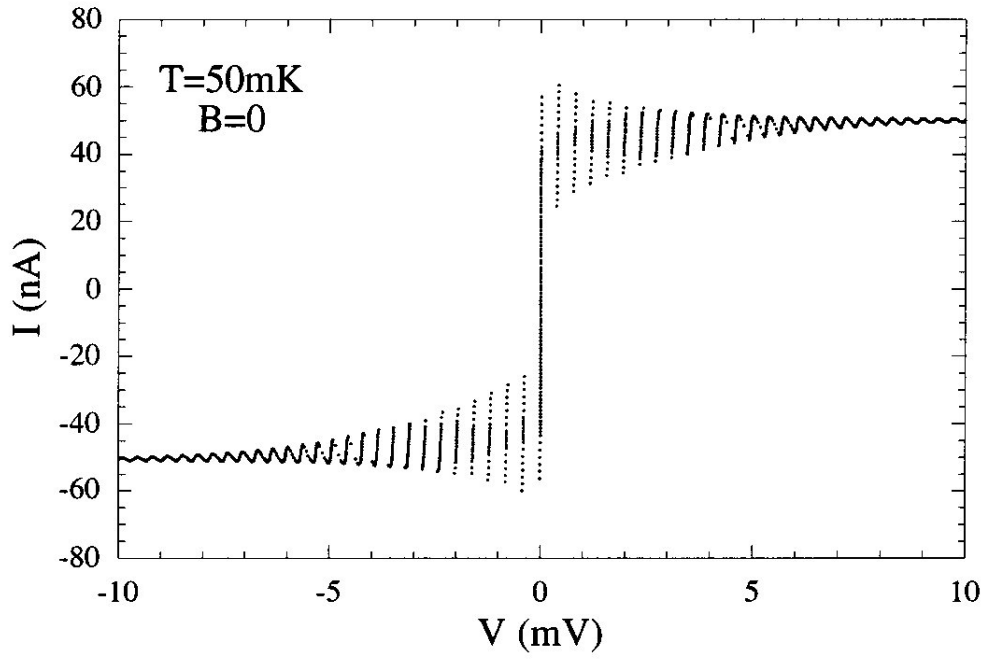

Figure 3.1: An experimentally obtained hysteresis curve for a 1D-array with 255 Josephson junctions. From Ref. [3], reprinted by permission of the author.

The voltage is related to the phase shift of the wave function as the current passes the Josephson junction. More exactly, the voltage $V = \frac{\hbar}{2e}\frac{d\varphi}{dt}$. This can be inserted into our derived Kirchoff's law equation to formulate an equation relating current to phase shift,

$$I = I_c \sin(\varphi) + \frac{\hbar}{2eR}\frac{d\varphi}{dt} + \frac{C\hbar}{2e}\frac{d^2\varphi}{dt^2}. \tag{3.3}$$

There is a more appropriate way to formulate Eq. (3.3) by making the equation dimensionless. This has the advantage that the number of dependent variables are decreased. With the substitution $\tau = \frac{1}{\tau_J}t$, where $\tau_J = \frac{\hbar}{2eRI_c}$, Eq. (3.3) becomes

$$\frac{I}{I_c} = \sin(\varphi) + \frac{d\varphi}{d\tau} + \beta_c\frac{d^2\varphi}{d\tau^2} \tag{3.4}$$

where $\beta_c = \frac{2eR^2CI_c}{\hbar}$.

3.2.1 The single junction problem

The single junction problem is a closed circuit with an external current flowing through a single Josephson junction. The problem is modeled using Eq. (3.4), which is solved for different variables β_c and $\frac{I}{I_c}$.

3.2.2 The 1D-array

Here we go through the steps to generalize he single junction problem into a problem with N Josephson junctions. As before, an external current runs through the circuit.

N Josephson junctions are connected in series, as shown by the schematics in Fig. 3.2. Different from the single junction problem is that there are capacitors connected between the Josephson junctions and connected to the current source.

This does not affect the Kirchoff's law formulation for the current through the first Josephson junction, Eq. (3.4) but it does alter the other equations.

A new equation can be formulated at the node connecting two next to each other lying Josephson junctions, junctions n and $n+1$ and a capacitor with capacitance C_0 using Kirchoff's law. Assume that the phase before Josephson junction n is θ_{n-1}, the phase between junction n and $n+1$ to be θ_n and the phase after junction $n+1$ is θ_{n+1}. The phase after the capacitor is θ_{end}.

We can expect phase shifts to be of importance, therefore we introduce $\varphi_n = \theta_n - \theta_{n-1}$ and $\varphi_{n+1} = \theta_{n+1} - \theta_n$.

The current entering this node, I_{in}, is the current through the Josephson junction n. Using Eq. (3.3),

$$I_{in} = I_c \sin(\varphi_n) + \frac{\hbar}{2eR}\frac{d\varphi_n}{dt} + \frac{C\hbar}{2e}\frac{d^2\varphi_n}{dt^2}, \tag{3.5}$$

while the current out of the node, I_{out}, is the current through junction $n+1$ and the current through the capacitor. The current I_{out} is then

$$I_{out} = I_c \sin(\varphi_{n+1}) + \frac{\hbar}{2eR}\frac{d\varphi_{n+1}}{dt} + \frac{C\hbar}{2e}\frac{d^2\varphi_{n+1}}{dt^2} + \frac{C_0\hbar}{2e}\frac{d^2(\theta_{end}-\theta_n)}{dt^2}. \tag{3.6}$$

As in section 3.2, Eq. (3.5) and Eq. (3.6) can be reformulated by introducing the variable τ and β_c. In the 1D-array problem, another variable is introduced, $\beta_{c0} = \beta_c \cdot \frac{C_0}{C}$. This gives, using $I_{in} = I_{out}$,

$$\sin(\varphi_n) + \frac{d\varphi_n}{d\tau} + \beta_c\frac{d^2\varphi_n}{d\tau^2} = \sin(\varphi_{n+1}) + \frac{d\varphi_n}{d\tau} + \beta_c\frac{d^2\varphi_{n+1}}{d\tau^2} + \beta_{c0}\frac{d^2(\theta_{end}-\theta_n)}{d\tau^2}. \tag{3.7}$$

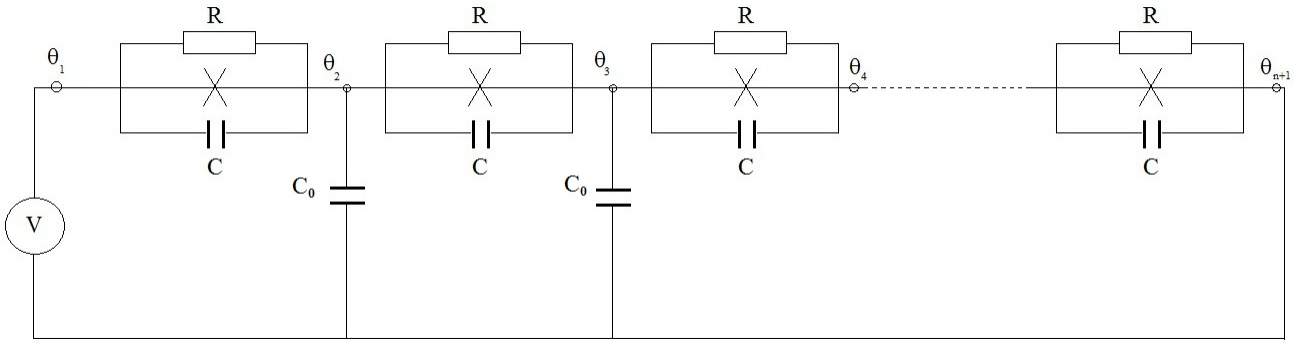

Figure 3.2: The 1D array of Josephson junctions. Between each set of Josephson junctions there is a capacitor of capacitance C_0.

3.3 Analytical Calculations

Eq. (3.4) and Eq. (3.7) are too complicated to be solved analytically. What can be done is an analysis of specific cases for the single Josephson junction problem, where we will look at the small-angle approximation and taking β_c in certain limits to see what can be said of the analytical solution in these cases.

3.3.1 Small angle approximation

One way of solving Eq. (3.4) or Eq. (3.7) is to assume that the phase shift φ is small. Then, the sinus can be approximated to a linear, first-order term, $\sin(\varphi) \approx \varphi$. While this gives a simple problem to solve (equivalent to a small-angle pendulum problem), it demands that the phase shifts are small. In our problem with Josephson junctions, this is not the case. Therefore we look to other approximations we can make to simplify the problem.

3.3.2 Overdamped solution

The solutions to Eq. (3.4) depend on the value of β_c. The simplest case is when the system is overdamped, that is $\beta_c << 1$. In that case Eq. (3.4) becomes $\frac{I}{I_c} = \sin(\varphi) + \frac{d\varphi}{d\tau}$ and the problem can be solved analytically. The dynamic solution to the problem is solved by variable separation

$$d\tau = \frac{d\varphi}{\frac{I}{I_c} - \sin(\varphi)}, \tag{3.8}$$

which can be looked up in an integral table, where it is found that the solution is

$$\varphi(t) = 2\arctan\left[\sqrt{1 - \left(\frac{I_c}{I}\right)^2}\tan\left(t\sqrt{\frac{(\frac{I}{I_c})^2 - 1}{2\tau_J}}\right) - \frac{I_c}{I}\right]. \tag{3.9}$$

This can then be integrated over time to determine the period of the solution of φ. By then using the Josephson frequency relation $2eV/\hbar = 2\pi/T$, we obtain the voltage-current relation

$$V = R(I^2 - I_c^2)^{1/2}. \tag{3.10}$$

Here we observe that the solution will be imaginary for $I < I_c$ and linear and real for $I >> I_c$. An imaginary voltage means that the voltage will be 90 degrees ahead of the current peak in a phase diagram. For a DC current this yields, such as in our case, a zero net voltage for $I < I_c$. No hysteresis can be observed by these calculations.

3.3.3 Underdamped solution

An underdamped solution is one where $\beta_c > 1$. This gives a non-linear second-order differential equation that cannot be solved analytically. What is obtained are several solutions that depend on which initial value was selected. That is, there is hysteresis: the solution can be different simply by changing the direction.

For example, the solution to Eq. (3.4), with $\beta_c > 1$, will depend on the current applied through the Josephson junction. If the initial current starts off below I_c, the circuit will be superconducting, and therefore there will be no resistance and no voltage drop. On the other hand, if the current is above I_c there will be resistance, but even if the current were to drop below I_c, there will still be resistance until the current has dropped off sufficiently. This hysteresis is plotted numerically and shown in section 3.5.

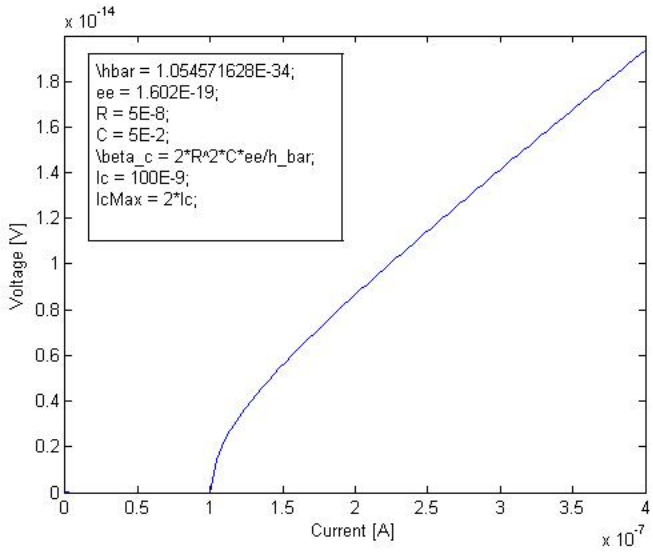

Figure 3.3: The I-V characteristics of the analytical solution of an overdamped Josephson junction.

3.4 Numerical Analysis

The numerical results in this report were obtained using Matlab. In section 3.2.2, a system of second-order differential equations were obtained. This can be turned into a system of first-order differential equations with a change of variables that can be solved using one of Matlab's ode-solvers. From this solution, the instantaneous voltage can be calculated as a function of external current. As only the average voltage is measurable, the Matlab function *time series* is used to average the phase shift so that the average voltage can be calculated. An I-V graph can then be plotted.

A constant β_c is chosen while the external current is increased from zero up to a given value lying above I_c before going down to zero again. Since we have eliminated the constants with the help of β_c we need not bother in these solutions with any values of R or C. When we plot the I-V characteristics we calculate the voltage as $V = \frac{\hbar}{2e}\frac{d\varphi}{d\tau}$, where the elementary charge $e = 1.602 \cdot 10^{-19}$ C and Planck's constant divided by 2π $\hbar = 1.05457 \cdot 10^{-34} \frac{m^2 kg}{s}$.

3.4.1 Single Josephson junction

The single Josephson junction problem, see Fig. 3.4 was solved using Matlab's solver *ode23s* foremost, but also *ode45*. The equation is first reformulated into a first-order differential equation with two unknown variables.

$$\xi_1 = \varphi, \qquad \xi_2 = \frac{d\xi_1}{d\tau} \qquad \rightarrow \qquad \xi = \begin{pmatrix} \xi_1 \\ \xi_2 \end{pmatrix} \tag{3.11}$$

Introducing this variable into Eq. (3.4) gives:

$$\frac{I}{I_c} = \sin(\xi_1) + \xi_2 + \beta_c \frac{d\xi_2}{d\tau}. \tag{3.12}$$

This is reformulated into $\mathbf{A}\dot{x} = \mathbf{B}x + \mathbf{C}$,

$$\begin{pmatrix} 1 & 0 \\ 0 & \beta_c \end{pmatrix} \frac{d\xi}{d\tau} = \begin{pmatrix} 0 & 1 \\ 0 & -1 \end{pmatrix} \xi - \begin{pmatrix} 0 \\ \sin(\xi_1) \end{pmatrix} - \frac{I}{I_c} \begin{pmatrix} 0 \\ 1 \end{pmatrix}. \tag{3.13}$$

Eq. (3.13) is set up using Matlab's command *function*. A Matlab script is created that takes ξ and t as input variables and returns the derivative $\frac{d\xi}{dt}$. This is then called to by ode23s, which solves the problem $\mathbf{A}\dot{x} = \mathbf{B}x + \mathbf{C}$.

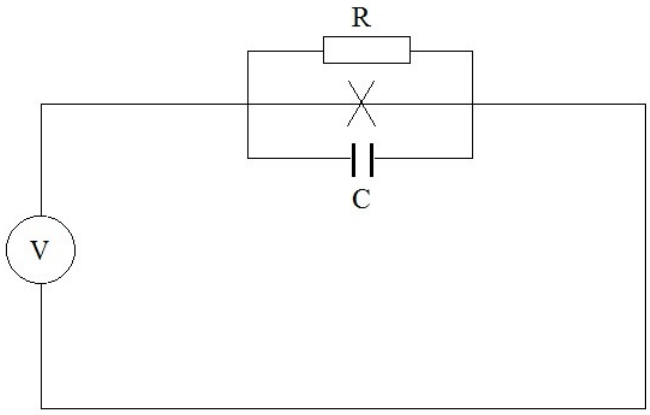

Figure 3.4: The single Josephson junction circuit which we began simulating.

The problem is solved in steps, where each step has a constant external current I. The external current is, stepwise, increased from zero up to a current above I_c, and then down to zero again. For each step, the ordinary differential equation is allowed to reach a steady-state solution by running a preordained length of time t. The I-V graph is plotted for different values of β_c and the results are noted.

3.4.2 1D-array of Josephson junctions

The problem with a 1D-array of Josephson junctions, is solved similarly to the single Josephson junction problem. It is solved using ode23s with input variables ξ and t and output variable $\frac{d\xi}{dt}$. Instead of the vector of the phase difference ξ, it is better to look at the phases themselves, due to the new term of $\theta_{end} - \theta_n$ entering Eq. (3.7).

Instead of considering ξ, the variable x is used. Changing from ξ to x results in two extra variables θ_{end} and $\dot{\theta}_{end}$ that are set to zero. As the problem only depends on the phase shifts and not the absolute value of the phases, one of the phases can be designated as a reference of constant phase, which we choose to be zero. For N Josephson junctions Eq. (3.4) is reformulated using

$$x_{2n-1} = \theta_n \qquad x_{2n} = \frac{d\theta_n}{d\tau} \rightarrow \qquad \mathbf{x} = \begin{pmatrix} x_1 \\ x_2 \\ \vdots \\ x_{2N} \end{pmatrix} \tag{3.14}$$

into the form

$$\mathbf{A}\dot{\mathbf{x}} = \mathbf{B}\mathbf{x} + \mathbf{C}(\mathbf{x}) + \mathbf{D} \tag{3.15}$$

The arrays $\mathbf{A}, \mathbf{B}, \mathbf{C}(\mathbf{x})$ and $\mathbf{D}$ depend on the number of Josephson junctions but follow a formula. $\mathbf{A}$ is

$$\mathbf{A} = \begin{pmatrix} 1 & 0 & 0 & 0 & 0 & 0 & 0 & 0 & 0 & \dots \\ 0 & -\beta_c & 0 & \beta_c & 0 & 0 & 0 & 0 & 0 & \dots \\ 0 & 0 & 1 & 0 & 0 & 0 & 0 & 0 & 0 & \dots \\ 0 & \beta_c & 0 & -2\beta_c - \beta_0 & 0 & \beta_c & 0 & 0 & 0 & \dots \\ 0 & 0 & 0 & 0 & 1 & 0 & 0 & 0 & 0 & \dots \\ 0 & 0 & 0 & \beta_c & 0 & -2\beta_c - \beta_0 & 0 & \beta_c & 0 & \dots \\ \vdots & \vdots & \vdots & \vdots & \vdots & \vdots & \vdots & \vdots & \vdots & \ddots \end{pmatrix}, \tag{3.16}$$

while $\mathbf{B}$ is

$$\mathbf{B} = \begin{pmatrix} 0 & 1 & 0 & 0 & 0 & 0 & 0 & 0 & 0 & \dots \\ 0 & 1 & 0 & -1 & 0 & 0 & 0 & 0 & 0 & \dots \\ 0 & 0 & 0 & 1 & 0 & 0 & 0 & 0 & 0 & \dots \\ 0 & -1 & 0 & 2 & 0 & -1 & 0 & 0 & 0 & \dots \\ 0 & 0 & 0 & 0 & 0 & 1 & 0 & 0 & 0 & \dots \\ 0 & 0 & 0 & -1 & 0 & 2 & 0 & -1 & 0 & \dots \\ \vdots & \vdots & \vdots & \vdots & \vdots & \vdots & \vdots & \vdots & \vdots & \ddots \end{pmatrix}. \tag{3.17}$$

The vectors $\mathbf{C}(\mathbf{x})$ and $\mathbf{D}$ are

$$\mathbf{C}(\mathbf{x}) = -\begin{pmatrix} 0 \\ \sin(\theta_3 - \theta_1) \\ 0 \\ \sin(\theta_5 - \theta_3) - \sin(\theta_3 - \theta_1) \\ 0 \\ \vdots \\ \sin(-\theta_{2N-1}) - \sin(\theta_{2N-1} - \sin(\theta_{2N-3}) \end{pmatrix} \qquad \mathbf{D} = \begin{pmatrix} 0 \\ \frac{I}{I_c} \\ 0 \\ 0 \\ \vdots \end{pmatrix} \tag{3.18}$$

When plotting the I-V curve, the voltage is observed as $\dot{\theta}_{end} - \dot{\theta}_1$, but since $\dot{\theta}_{end} = 0$, $-\dot{\theta}_1$ is the only variable used.

3.5 Results

3.5.1 Single Josephson junction

The single Josephson junction problem is solved for different values of β_c. The values are chosen from very low β_c values, $\beta_c = 10^{-4}$ up to very large β_c values, $\beta_c = 10^4$. In this thesis, most focus was put on β_c values around 10. Plotted in Fig. 3.5 and Fig. 3.6 are solutions with β_c values of 10 and 0.1 respectively.

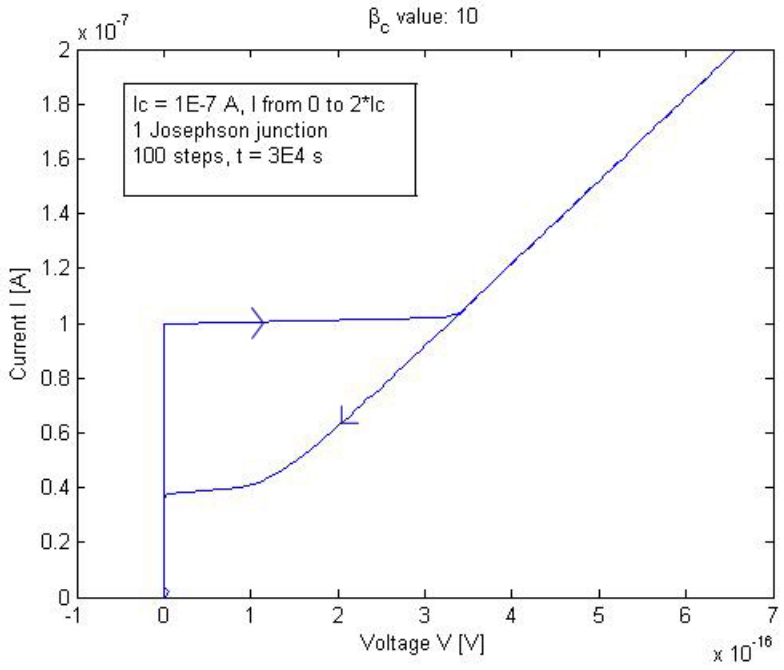

Figure 3.5: Hysteresis in the I-V curve for a single Josephson junction.

3.5.2 1D-array of Josephson junctions

Numerical analysis for different number of Josephson junctions were carried out. In Fig. 3.7 and Fig. 3.8 the current I versus V is plotted for 2 and 250 Josephson junctions respectively, both with β_c-value of 10.

The curves have the same overall shape, differing only in the voltage scale. The numerical solver needed a larger value of the variable t_{tot} in Fig. 3.8 than in Fig. 3.7, $3 \cdot 10^5 s$ compared to $5 \cdot 10^4 s$. t_{tot} is the time over which the solution was calculated in the program, note that it is not the actual time for solving the differential equations.

Another difference is the slope when the current is just increased passed $I_c = 10^{-7} A$. The slope for three Josephson junctions is flatter than the one for 250 Josephson junctions.

The instability of the hysteresis solution near $I = 0$ in Fig. 3.6 is an inherent trait to our solver for low times, regardless of the number of circuits. For large numbers however, the solution is stable. To account for this we derived another mass matrix $\mathbf{A}$, in order to rewrite the problem. The problem was only rewritten, so the solution was kept the same, as can be seen in Fig. 3.7, which is a graph obtained from the new mass matrix. This alternate program is more stable at the cost of longer solving time. It quickly becomes untenable with increasing number of Josephson junctions.

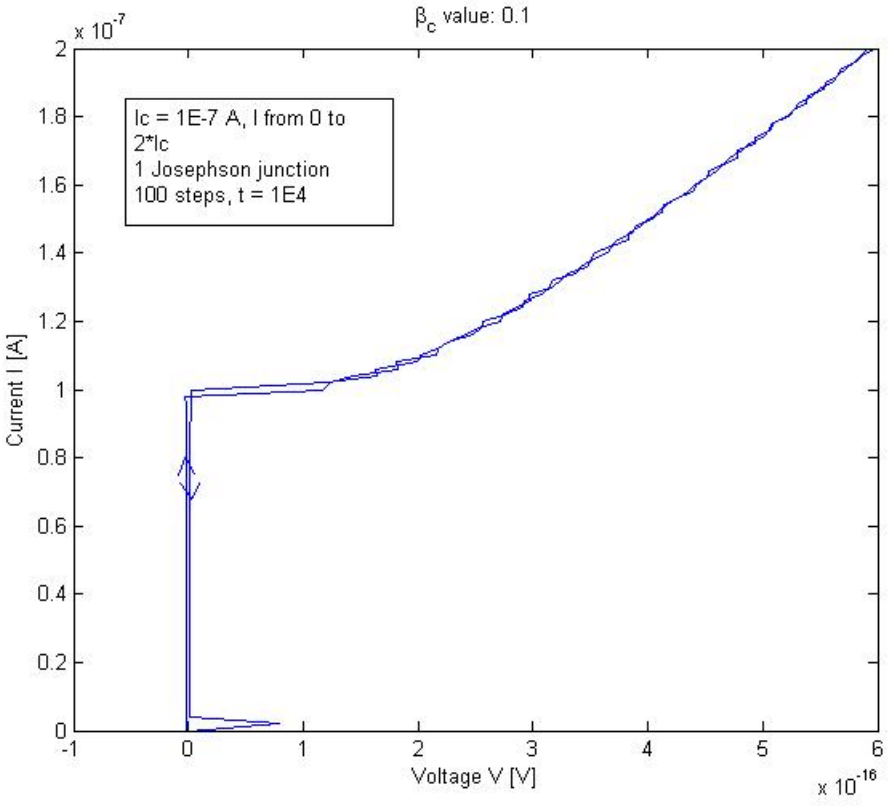

Figure 3.6: Hysteresis single Josephson junction.

It was noticed that voltage changed with the number of Josephson junctions. Therefore the relationship between the voltage and the number of Josephson junctions is plotted in Fig. 3.9. The voltage that is plotted is the difference in voltage when the external current is slightly above and below the critical current I_c, in the case when $B_c = 10$.

The slope for different values of β_c and the critical current, I_c, is evaluated in Table 3.1. Only the slope is analyzed, since we do not consider the voltage-intercept to be of interest. The linear regression is determined for 4, 8, 12 and 16 Josephson junctions, making it a rough evaluation. From the data it seems that I_c does not affect the slope. The data for different β_c values are inconclusive, so a slightly more in-depth evaluation is done, the results displayed in Table 3.2.

		I_c value [A]			
		10^{-5}	10^{-6}	10^{-7}	10^{-8}
β_c value	2	0.3632	0.3632	0.3632	0.3632
	6	0.3740	0.3740	0.3740	0.3740
	10	0.3747	0.3747	0.3747	0.3747
	14	0.3737	0.3737	0.3737	0.3737

Table 3.1: The slope for a linearly regressed solution relating voltage jump and number of Josephson junctions for different β_c values and critical currents I_c. The noted values are of order 10^{-15}.

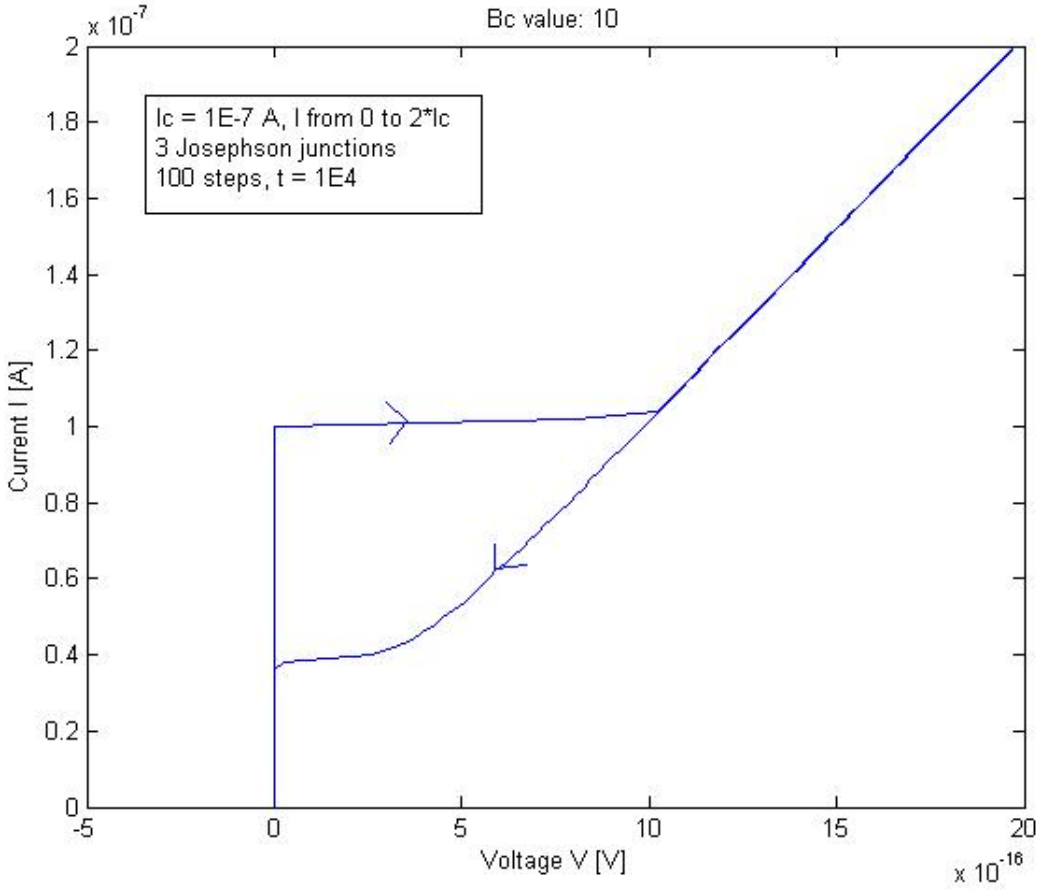

Figure 3.7: Three Josephson junctions.

		I_c value [A]
		10^{-7}
β_c value	20	0.3742
	24	0.3741
	28	0.3740
	32	0.3745

Table 3.2: The slope for a linearly regressed solution relating voltage jump and number of Josephson junctions for additional β_c values and critical current $I_c = 10^{-7}$ A. The noted values are of order 10^{-15}.

3.6 Discussion

As can be seen in the figures in section 3.5, the general shape of an I-V curve for N Josephson junctions connected in a series is the same as that of an I-V curve for a single Josephson junction. There are some differences though, that will depend on the number of Josephson junctions, and on the time for each step that is calculated before a solution is considered stable. It can be noted that the I-V characteristics obtained from our simulations agree by the overall shape, to I-V curves obtained experimentally. For instance Fig. 3.1, although it is not a hysteresis curve, shows the same shape as the

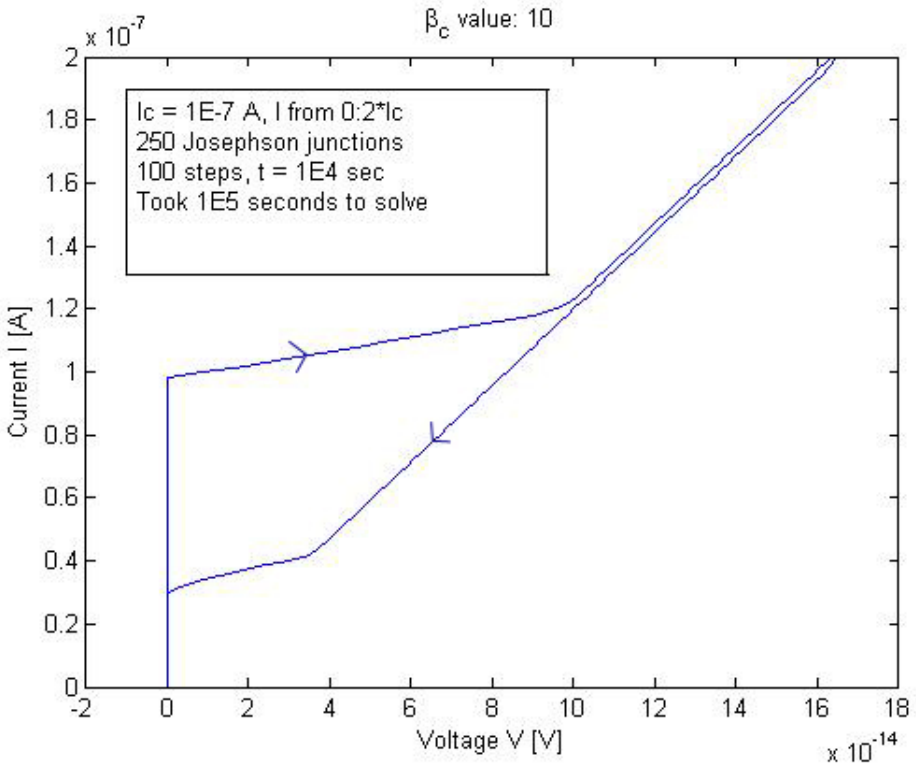

Figure 3.8: 250 Josephson junctions.

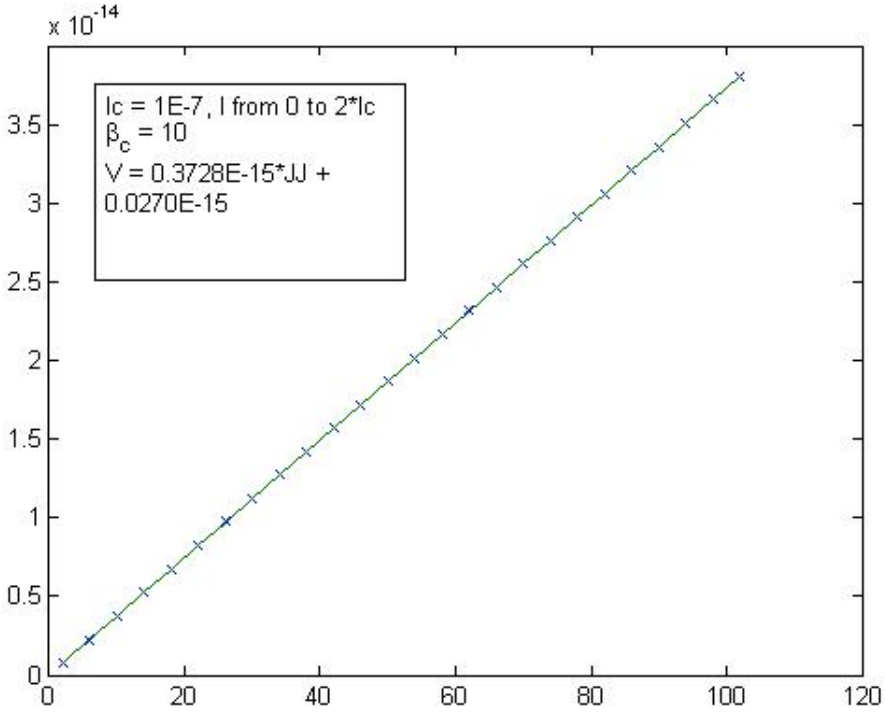

Figure 3.9: Number of Josephson junctions versus voltage jump. The "x" are measured data and the "-" are interpolated points.

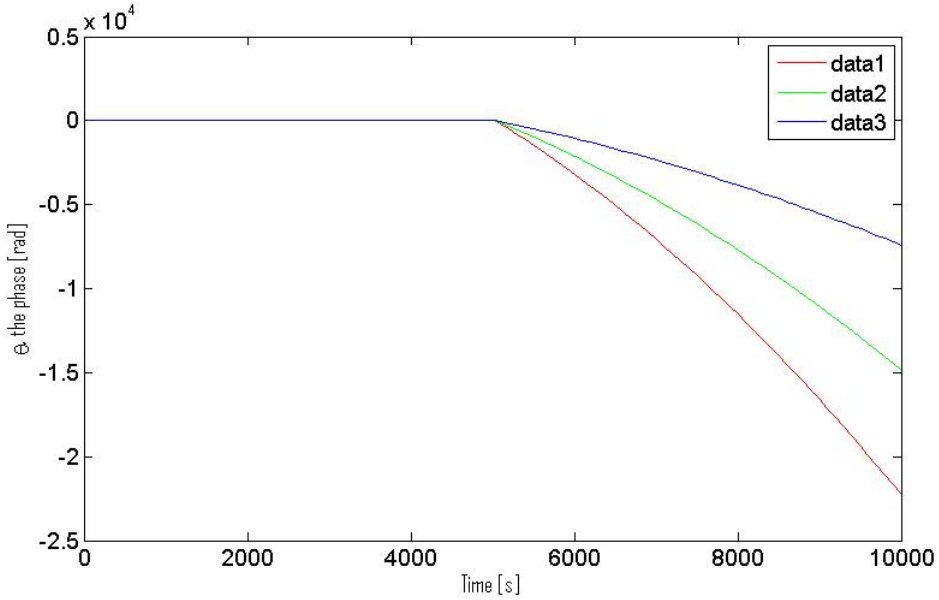

Figure 3.10: The three nonzero phases in a three Josephson junction array.

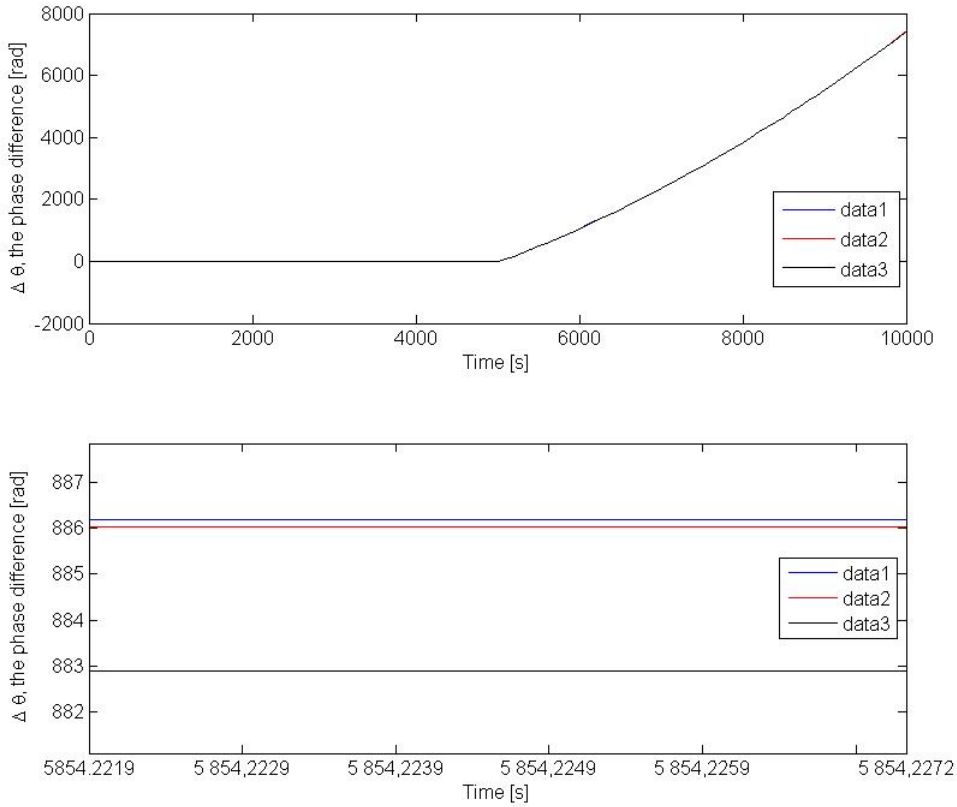

Figure 3.11: The phase difference over the three junctions in a three Josephson junction array.

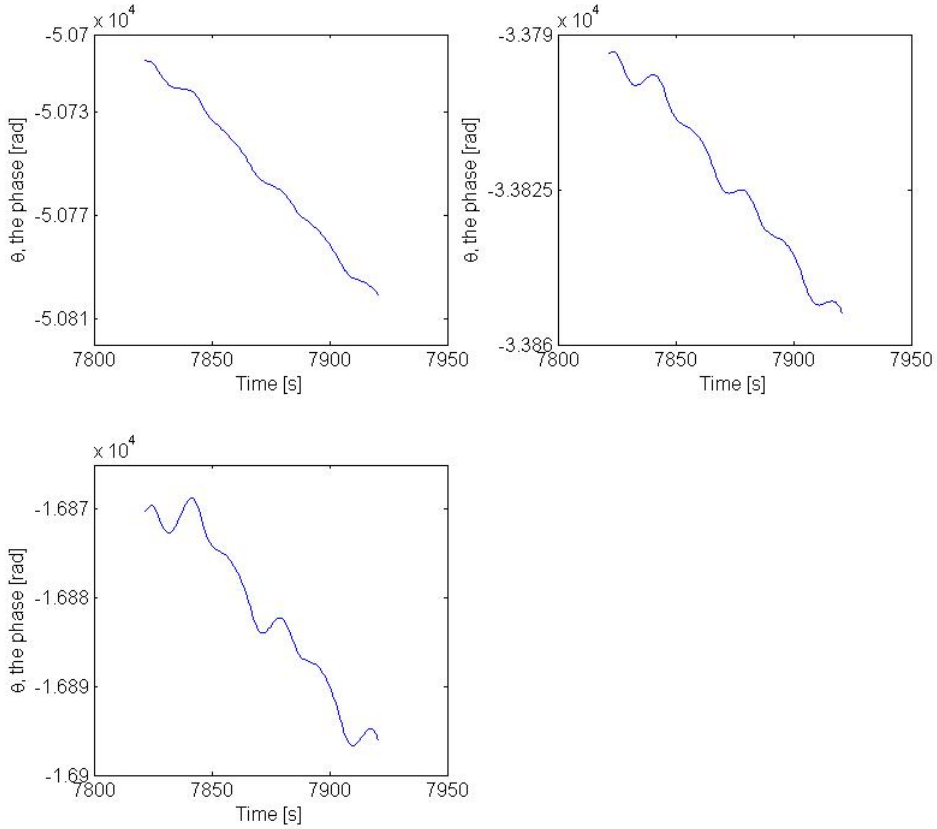

Figure 3.12: The three nonzero phases in a three Josephson junction array, zoomed in over step 80 of 101 of the solution.

graphs we have obtained by simulations in our thesis.

The first effect of replacing a single junction with a 1D-array is a general instability in the I-V curve. We have only shown some instability in one figure in this thesis, Fig. 3.6, when both current and voltage is near zero.

The second effect can most clearly be seen when comparing Fig. 3.8 and Fig. 3.5. There is a difference in slope for the I-V curve for currents larger than I_c. By increasing the total time, the slope flattens out. At the limit (when time $t \to \infty$), it can be expected that the slope would be completely flat, that the I-V curve, when the current is larger than I_c, jumps from the superconducting solution to the resistive solution. Since we are conducting numerical calculations, the time, t, is only chosen as a large number and the slope is not entirely flattened out. This is again in analogue with the tilted washboard model, where we need to let the mass come to rest in the slope before continuing to incline the plane further in order to obtain a solution only based on the incline of the plane and not on how fast it is tilted (the mass will otherwise gain a velocity to take it over the next top). This is no explanation nor is it intended as such, it is simply a conceptual analysis that can be applied to the numerical solutions of our problem. The real time of our simulations have varied from 10 s up to 28 h, from simulating one Josephson junction up to 250 Josephson junctions.

Increasing the number of junctions increases the number of coupled equations to be

solved, see section 3.2.2. This increases the time taken to solve the problem numerically, but otherwise, the shape of the solution is the same as for a single Josephson junction. What changes is the voltage for the resistive solution, the solution when the current is larger than I_c. The relationship between this voltage and the number of Josephson junctions is plotted in Fig. 3.9.

The plotted voltage is the one corresponding to the current $I = 1.14 \cdot I_c$. The reason that we plot the voltage for an I such that $I > I_c$ is that the jump between the superconducting and resistive solution is not instantaneous. The slope is also dependent not only on the total time of the solver, but also on the number of Josephson junctions in the array. This implies that for an increasing number of Josephson junctions, there needs to be an increase in total time for the solution, in order to obtain the same slope as for a smaller number of Josephson junctions. We assumed that an increase of 10^3 s per junction, along with taking the voltage at $I = 1.14 \cdot I_c$, was enough to ensure similar results for up to 100 junctions.

The reason that we measure from a current that is 14% increased from the critical current, I_c, is that we want margins to the theoretical current for the jump in voltage. The 14% was chosen arbitrary.

The increase in voltage is linear with increasing Josephson junctions. If a linear regression is made on the measurement results in Fig. 3.9, we see that the voltage V can be expressed as a function of Josephson junctions JJ by the equation

$$V = 0.3728 \cdot 10^{-15} \cdot JJ + 0.0270 \cdot 10^{-15}. \tag{3.19}$$

We should be able to extrapolate these results to an experimental case with 2400 Josephson junctions. For 2400 Josephson junctions, there is a voltage jump of about $895 \cdot 10^{-15}$V according to our extrapolation. This differs from the experimental results, as they are of the order of nV. This may be due to some other configuration in the experimental setup, for example a resistor in series with the junctions. It is also possible that this is partly due to quantum effects not regarded in our numerical models.

We also studied whether the parameters β_c and critical current, I_c, had any effect on the jump. We conclude that the jump is independent of I_c. For β_c however, we observe a slight fluctuation in the slope, depending on the β_c. Since the fluctuations due to β_c are very small and since the data we have gathered show no distinct relation between β_c and the size of the jump, we cannot conclude if there exists a relation. However, the results seems to indicate that there is no relation between the jump and the value of β_c. The small variation found for different β_c could then be perturbations with negligible effect on the value of the jump.

We have used a semi classical model in our work. What effects does this mean that we are overlooking and what consequences does it have on our solutions? There are mainly two things that we neglect in our problem compared to reality; quantum tunneling through potentials (not the insulators), and thermal noise. The first effect means that we have a spontaneous break of the superconductivity in some circuits due to quantum phenomenas and voltage will occur even though we have not reached the critical current. How this can be depicted is that the mass in the tilted washboard model would tunnel through a top that stops it from moving, and in fact that is a very good model.

The second effect, thermal noise, also introduces the system with stochastic properties very much like the neglected spontaneous break of superconductivity. When plotting an I-V characteristic of an array of Josephson junctions with hysteresis we have more than

one solution to our system of differential equations, this is what gives us the hysteresis. We have one solution for the increasing current and another solution is occupied at the retrapping current for instance. The thermal fluctuations can then push the solution between the possible different solutions, thus giving a more interesting behavior to the I-V characteristics. In this manner a distribution of different currents will be obtained and a mean value of the current can be acquired.This yields that a system of Josephson junctions, under influence of thermal noise, increases the retrapping current I_r and decreases the critical current I_c. Ref. [6](ch 6.3.3) The effect of thermal noise can be added into the equations, creating a system of stochastic differential equations, to solve.

The phase of the wave function of the *Cooper pairs* can also be examined. One can visualize these phases in various ways to see if they behave as expected. This was particularly done for a three Josephson junction array. Fig. 3.10 shows the three nonzero phases θ_1, θ_2 and θ_3. These are not the same, nor should we expect them to be since we would have no current if that was that case. From Fig. 3.11 we see that the phase difference over each Josephson junction is almost the same, which means that the voltage drop is almost the same over all junctions as well. Since there is a voltage drop over the grounded capacitors we do not expect the phase to be exactly the same over all junctions. This is confirmed by the observation that *data3* in Fig. 3.11, corresponding to $-\theta_3$, is clearly disconnected from *data2* and *data1*, representing $-\theta_1$ and $-\theta_2$.

There is a phenomena that is not the main scope of this thesis, that is referred to as *phase slip*, which is when a phase suddenly slips back some radians. Without going into what really occurs we still looked for it in our solution to see if our numerical solutions take this into account. As of Fig. 3.10 it seems as if it does not. When peering closer by plotting the phase in every time step over one step of the solution, step 80 of 100, Fig. 3.12 is acquired. It is hard to tell whether these phase plots contains the phase slips one would expect or not; they are not making sharp, well defined turns, even though they tend to oscillate weakly in a stochastic manner. We evaluated steps 30, 50, 52, 70, 98 and 100 as well and the general trend was that an increasingly oscillating behavior in the phases was perceived. We draw no conclusion on this subject other than that we observe some fluctuations in the phases and that it would take more extensive studies to deduce a more thorough result.

Over all, our results seems to agree with what can be expected from our setup, to the extent we have examined it. The exception is the possibly absent phase slips. The reason for this we do not know; it is possible that they eluded us by chance, that we have misinterpreted data or perhaps that they are not taken into account by numerical solutions.

Chapter 4

Summary and Conclusions

The aim of this Bachelor thesis was to investigate the I-V characteristics of Josephson junctions connected in series. A semi-classical model was used and numerical analysis carried out using direct current to calculate the current and voltage, by solving coupled, non-linear, second-order differential equations.

Some analytical analysis was possible for the single Josephson junction case, as the differential equation explaining the current behavior is exactly the same as the real pendulum problem. But for most cases, even for the single Josephson junction case, numerical analysis was required.

We analytically rewrote the second-order differential equations to first-order differential equations. These were then solved using Matlab and I-V curves were plotted. Mostly, the I-V curves were plotted for a β_c value of 10, where hysteresis occurs.

The results that were obtained corresponded to what was expected theoretically and mostly to what has been found experimentally. The I-V curve jumps between a superconducting solution and a resistive solution as the current increases passed the critical current. When starting with the superconducting solution and a current below the critical current, this jump between solutions occurs the moment the current passes its critical value. This is modified to a steep slope instead depending on the solving time when solving numerically.

The size of the jump across the voltage is growing with an increasing number of Josephson junctions. This relationship is linear up to a hundred junctions, which was the extent our survey of this phenomena, as larger circuit systems required a too large computational capability. We also studied whether the parameters β_c and critical current, I_c, had any effect on the jump. We conclude that the jump is independent of I_c. For β_c we can draw no certain conclusions. However, the results seems to indicate that there is no relation between the jump and the value of β_c.

The model is of semi-classical nature and is thus limited in its application to the Josephson junction. In the real case there are stochastic properties from thermal noise and quantum tunneling that allows a nonzero voltage across a superconductor.

We have also not seen any phase slips for our phases, which we expected to see. Otherwise, the phases behaved as predicted, with there being no phase change for supercurrents while the phase shifted for resistive currents in near equal spread between Josephson junctions. There was also an increase in phase shift with increasing resistive current, which corresponds to increasing voltage with increasing current.

Acknowledgments

We would like to thank our Supervisor Jack Lidmar and our supervisor Patrik Henelius for their moral support. Jack Lidmar helped us with conceptually understanding the quantum effects we were dealing with as well as guiding us when we were conducting our numerical calculations. Patrik Henelius has helped us with writing our thesis.

We would also like to thank David Haviland and his group for letting us use some of their material as a base for our thesis, which we have used to discuss the validity of our simulations.

Bibliography

[1] P. W. Anderson and J. M. Rowell *Probable Observation of the Josephson Superconducting Tunneling Effect*, Phys. Rev. Lett. 10, 230–232 (1963)

[2] S. Corlevi, *Quantum effects in nanoscale Josephson junction circuits*, PhD Thesis, KTH , Institution of theoretical physics, ISBN 91-7178-353-9 (2006)

[3] D. B. Haviland, K. Andersson, P. Ågren, *Superconducting and Insulating Behavior in One-Dimensional Josephson Junction Arrays*, Journal of Low Temp. Phys. vol. 118 (2000)

[4] B. D. Josephson, *Possible new effects in superconductive tunneling*, Phys. Lett. 1, number 7, (1962)

[5] C. Kittel, *Introduction to solid state physics 8th ed*, John Wiley & Sons, ISBN 0-471-41526-X, 289-290, (2005)

[6] M. Tinkham, *Introduction to superconductivity, 2nd ed*, Mcgraw-hill, ISBN 0-07-064878-6, (1996)